# Supporting Information

## Takasaki et al. 10.1073/pnas.1310777111

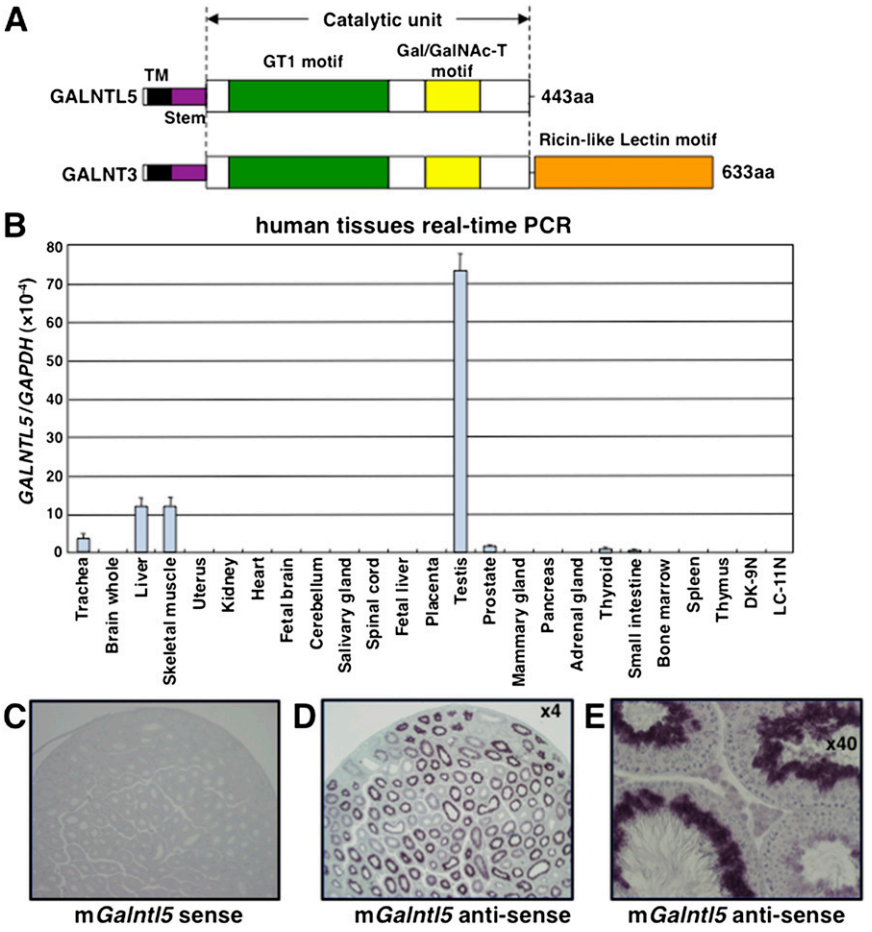


**Fig. S1.** Structure of human polypeptide *N*-acetylgalactosaminyltransferase-like protein 5 (GALNTL5) and expression patterns of the transcripts in human tissues and mouse testis. (*A*) Schematic comparison of human GALNTL5 [443 amino acids (aa)] and polypeptide *N*-acetylgalactosaminyltransferase protein 3 (GALNT3) (633 aa). Except for the truncation of the lectin domain (orange box), GALNTL5 has the motifs typical of the pp-GalNAc-gene family: transmembrane domain (TM, black), stem region (stem, purple), and a catalytic unit consisting of a GT1 motif (green) and a Gal/GalNAc-T motif (yellow). The structure of GALNT3 is shown for comparison. (*B*) Quantitative analysis of *GALNTL5* transcripts in human tissues and two human cell lines. The relative amount of *GALNTL5* transcripts was determined after normalization to glyceraldehyde-3-phosphate dehydrogenase (*GAPDH*). Values are the number of copies measured against *GAPDH* in 1 μg of total RNA. Bars represent the SEM of three independent experiments. In situ hybridization of sections of mouse adult testis with sense strand (*C*) and antisense RNA strands with the mouse *Galntl5* ortholog (*D* and *E*). Photomicrographs were taken with 4× (*C* and *D*) and 40× (*E*) lens objectives.

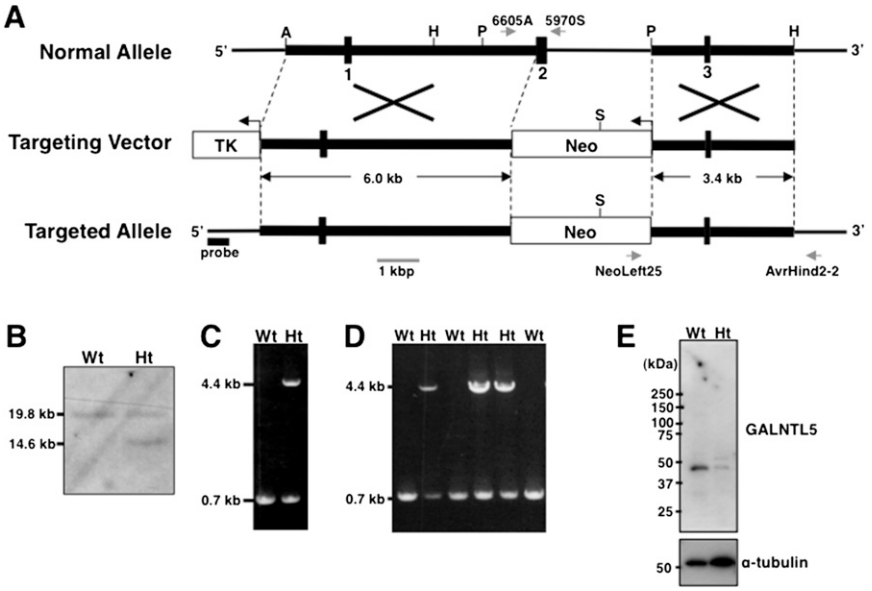


**Fig. S2.** Generation of mice lacking *Galntl5*. (*A*, *Top*) Normal allele showing the first three of the nine exons comprising mouse *Galntl5*. (*Middle*) Targeting construct with the neomycin resistance gene (Neo) and the thymidine kinase gene (TK) as selectable markers. Homologous recombination occurred with 6.0-kbp and 3.4-kbp regions encompassing the first and third exons, respectively. (*Bottom*) The targeted allele, where the second exon, including the translational start site, has been replaced with a Neo cassette. Numbered boxes indicate exons, thick horizontal lines represent homologous DNA regions, and bars and gray arrows indicate the positions of the 5′ probe and the PCR primers (6605A, 5970S, NeoLeft25, and AvrHind2-2), respectively. Restriction enzyme sites are indicated by A (AvrII), H (HindIII), P (PmlI), and S (SpeI). (*B*) Genotyping of wild-type (WT) and heterozygous (Ht) ES cells with Southern blot analysis of genomic DNA hybridized using the 5′ flanking probe. After digestion with SpeI, the probe detected 19.8-kb and 14.6-kb fragments as the normal and targeted alleles, respectively. (*C*) Genotyping of embryonic stem cells with PCR by using four primers. A 0.7-kb DNA fragment from the normal allele and a 4.4-kb DNA fragment from the targeted allele were amplified. (*D*) Genotyping of mice by means of PCR of DNA purified from mice tails. WT and Ht offspring were born from the mating of Ht females and WT males because the Ht male mice were sterile. (*E*) Comparison of GALNTL5 in epididymal sperm from WT and Ht mice.

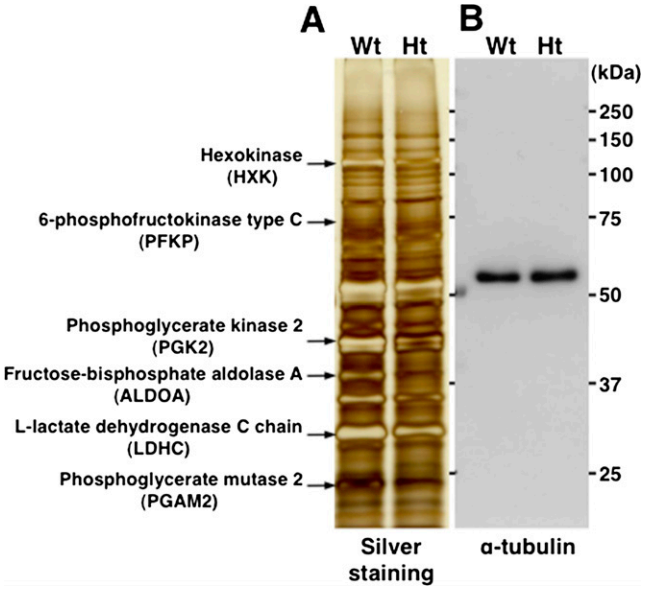


**Fig. S3.** Protein compositions of epididymal spermatozoa of WT and Ht male mice. (*A*) Protein identification by MS/MS analysis. Quantitative differences of the proteins from the sperm of each male genotype were assessed by using SDS/PAGE with silver staining. Mass spectroscopy identified six glycolytic enzymes from each of the silver-stained bands (arrows). (*B*) α-Tubulin served as the control. Protein standards are shown on the *Right*.

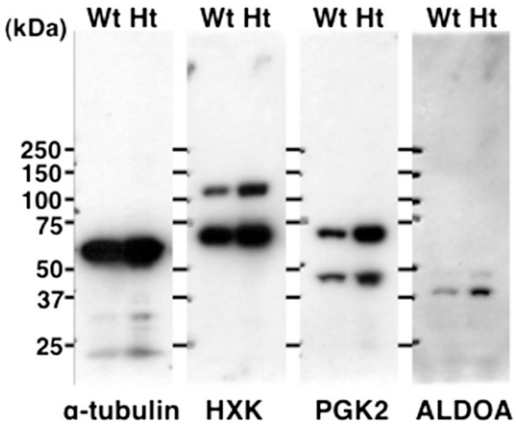


**Fig. S4.** Detection of glycolytic enzyme protein components in mouse testes. Testis lysates were separated by SDS/PAGE and blotted with antihexokinase (HXK), antiphosphoglycerate kinase 2 (PGK2), and anti–fructose-bisphosphate aldolase A (ALDOA) antibodies. The amount of each isozyme in the testis was equal between WT and Ht mice. α-Tubulin served as the control. Protein standards are shown on the *Left*.

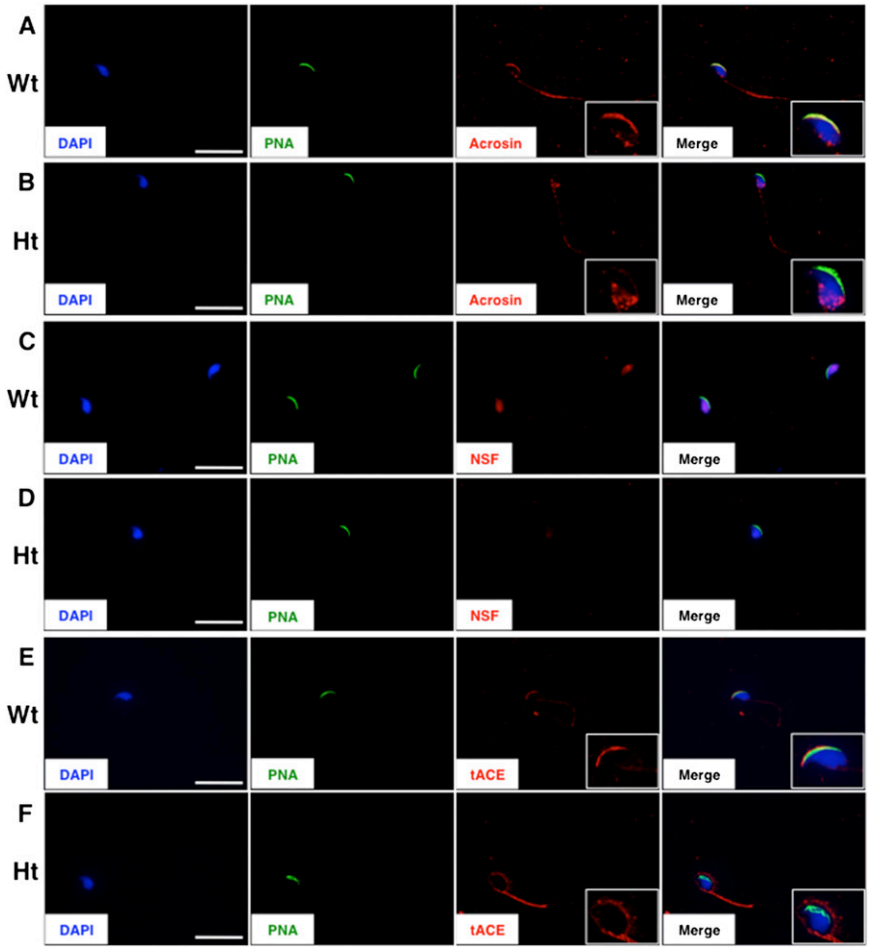


**Fig. S5.** Immunostaining of sperm with an antiacrosin antibody, an anti– *N*-ethylmaleimide-sensitive factor (NSF) antibody, and an anti–testicular angiotensin-converting enzyme (tACE) antibody. Immunostaining of sperm from WT mice (*A*) and Ht mice (*B*) with an antiacrosin antibody. Acrosin signals are present in the acrosome of sperm from WT mice. Signals are weak in the acrosomes of sperm from Ht mice. *Insets* are close-ups of sperm heads. NSF signals are detected in the heads of epididymal sperm of WT mice (*C*), but are not or only weakly detected in the heads of epididymal sperm of Ht mice (*D*). Signals are observed on the outer membrane of the acrosome and weakly observed in the middle region of the tail in sperm of WT mice (*E*). In sperm of Ht mice, the signals are aberrantly present on the plasma membrane surrounding the head and the middle tail region (*F*). Peanut agglutinin (PNA) and DAPI stain the acrosome and the nuclei, respectively. (White scale bars, 20 μm.)

**Table S1. Clinical semen analyses**

| Sample no. | Semen volume, mL | Sperm concentration, $\times 10^6$/mL | Sperm motility, % | Sperm normal morphology, % | Abnormalities |
|---|---|---|---|---|---|
| 1 | 4.9 | 86 | 55.8 | 23.1 | Normal |
| 2 | 4.1 | 46 | 56.5 | 20.9 | Normal |
| 3 | 4.1 | 252 | 68.3 | 22.2 | Normal |
| 4 | 2.4 | 148 | 58.1 | 20.9 | Normal |
| 5 | 2.1 | 63 | 19 | 6.7 | Asthenozoospermia |
| 6 | 6.6 | 29 | 0.3 | 7.2 | Asthenozoospermia |
| 7 | 3.6 | 21 | 21.6 | 5.6 | Asthenozoospermia |
| 8 | 5 | 13 | 28.8 | 10.9 | Asthenozoospermia |
| 9 | 5.5 | 49 | 8.2 | 1.8 | Asthenozoospermia |